How Hormone Receptor–DNA Binding Affects Nucleosomal DNA: The Role of Symmetry

Thomas C. Bishop, Dorina Kosztin, and Klaus Schulten*
Beckman Institute, Departments of Chemistry and Physics, University of Illinois at Urbana-Champaign, Urbana, Illinois 61801 USA

ABSTRACT Molecular dynamics simulations have been employed to determine the optimal conformation of an estrogen receptor DNA binding domain dimer bound to a consensus response element, ds(AGGTCACAGTGACCT), and to a nonconsensus response element, ds(AGAACACAGTGACCT). The structures simulated were derived from a crystallographic structure and solvated by a sphere (45-Å radius) of explicit water and counterions. Long-range electrostatic interactions were accounted for during 100-ps simulations by means of a fast multipole expansion algorithm combined with a multiple time-step scheme in the molecular dynamics package NAMD. The simulations demonstrate that the dimer induces a bent and underwound (10.7 bp/turn) conformation in the DNA. The bending reflects the dyad symmetry of the receptor dimer and can be described as an S-shaped curve in the helical axis of DNA when projected onto a plane. A similar bent and underwound conformation is observed for nucleosomal DNA near the nucleosome's dyad axis that reflects the symmetry of the histone octamer. We propose that when a receptor dimer binds to a nucleosome, the most favorable dimer-DNA and histone-DNA interactions are achieved if the respective symmetry axes are aligned. Such positioning of a receptor dimer over the dyad of nucleosome B in the mouse mammary tumor virus promoter is in agreement with experiment.

INTRODUCTION

Approximately 80% of the DNA in a cell nucleus is packed into nucleosomes (Noll, 1974), and therefore accessing DNA for the purpose of gene expression requires a local rearrangement of nucleosomes. Various molecular mechanisms have evolved to accomplish this rearrangement. One such mechanism is the hormone response mechanism (Beato et al., 1995), for which a satisfactory model has yet to be found (Beato et al., 1996b).

The nucleosome is a well-defined protein-DNA complex containing 146 bp of DNA wrapped 1.75 turns around a cylindrical complex of eight histones (Finch et al., 1977; Richmond et al., 1984; Arents et al., 1991), as represented schematically in Fig. 1. The histone octamer is dyad symmetrical (Richmond et al., 1984), and the point where the axis of symmetry intersects nucleosomal DNA, the dyad, divides the DNA into two symmetrical regions. At the dyad, the minor groove of the DNA is preferentially directed away from the surface of the histone octamer and defines a rotational phasing of the major and minor groove of the DNA on the histone octamer (Travers, 1987).

In a region extending 1.5 helical turns to either side of the dyad, the helix repeat is 10.7 bp/turn; farther away from the dyad, the helix repeat is 10.0 bp/turn (Hayes et al., 1990; Puhl and Behe, 1993). Regularly spaced sites on the surface of the histone octamer allow favorable interactions with the DNA backbone that correspond to the values of helix repeat, described above, and that define a translational positioning of DNA on the histone octamer. The boundaries between regions of differing helix repeat coincide with bends in the DNA that create an S-shaped bend in the path of the DNA, as indicated in Fig. 1. The resulting conformation of nucleosomal DNA reflects the dyad symmetry of the histone octamer (Richmond et al., 1984; Arents et al., 1991) because a matching symmetry allows the greatest number of favorable histone-DNA interactions. Intrinsically bent sequences of DNA that disrupt the interactions can be employed in vitro to affect a rotational and translational positioning of nucleosomal DNA on the histone (Travers, 1987; Sivolob and Khrapunov, 1995).

Regulation of gene expression by the hormone response mechanism relies on the ability of DNA binding proteins (hormone receptors) to bind with high affinity to target sequences of DNA (hormone response elements) and to alter the local arrangement of nucleosomes in chromatin (Beato et al., 1996a; Mymryk and Archer, 1995; Truss et al., 1995). A single subdomain of the hormone receptor determines the DNA sequence to which a hormone receptor dimer binds (Freedman et al., 1988); this subdomain is called the DNA-binding domain (DBD).

Hormone receptors typically bind as dimers to a hormone response element such that the protein-DNA complex is dyad symmetrical. The dyad symmetry of an estrogen receptor (ER) DBD dimer/DNA complex can be discerned from a representation of the corresponding crystallographic structure presented in Fig. 2. The DNA in the crystallographic structure is a consensus estrogen response element (ere), ds(|AGGTCA|CAG|TGACCT|), possessing the same symmetry as the dimer. Here, the vertical bars delineate two 6-bp sequences that are recognized by each monomer. Each

Received for publication 18 September 1996 and in final form 31 January 1997.

Dr. Bishop's current address: Department of Chemistry, University of California, Berkeley, CA 94720-0001.

Address reprint requests to Dr. Klaus Schulten, Department of Physics, Beckman Institute 3147, University of Illinois, 405 N. Mathews Ave., Urbana, IL 61801. Tel.: 217-244-2212; Fax: 217-244-6078; E-mail: kschulte@ks.uiuc.edu.

0006-3495/97/05/2056/12 $2.00

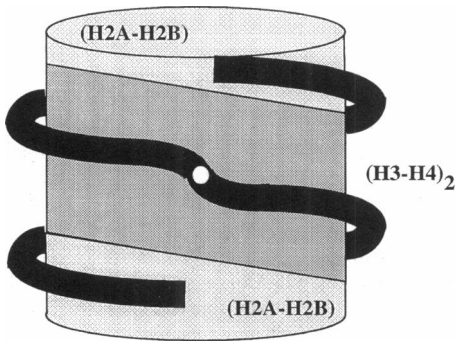

FIGURE 1 Schematic representation of a nucleosome. A nucleosome consists of a protein core of eight histones (*cylinder*) around which is wrapped the DNA (*solid line*). The histone octamer is a tripartite assembly of two (H2A-H2B) dimers and an $(H3\text{-}H4)_2$ tetramer that is dyad symmetrical. A white dot indicates the point where the axis of dyad symmetry intersects the DNA. An S-shaped bend in the helical axis of the DNA is observed in this region.

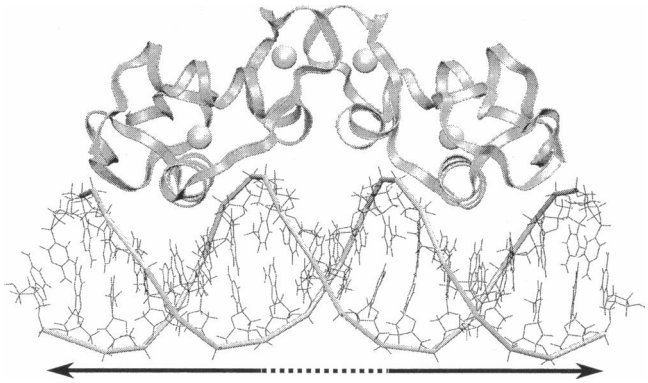

FIGURE 2 Representation of the ER-DBD dimer/DNA complex. Each monomer is represented as a ribbon, and the DNA is represented by lines. Spheres represent the two zinc ions associated with each monomer. The two half-sites and the spacer are indicated by arrows and a dotted line, respectively. This image has been created with VMD (Humphrey et al., 1996).

hexamer is referred to as a half-site, and the 3 bp between the half-sites constitute the spacer. The properties of B-form DNA are such that the major groove of each half-site and the minor groove of the spacer appear on the same face of the response element.

The so-called reading helix of each monomer recognizes each half-site primarily through interactions in the major groove. The reading helices are directed into and out of the page in Fig. 2. The resulting protein-DNA binding motif ensures that a hormone receptor dimer can bind to one face of the DNA and, hence, to nucleosomal DNA.

One expects that optimal interactions of the ER-DBD dimer in the major groove require the conformation of the DNA to reflect the dyad symmetry of the dimer (Bishop and Schulten, 1996). In fact, the symmetry existing in some DNA-binding proteins has been utilized to predict a structure for the corresponding protein-DNA complex by means of molecular modeling (Sandmann et al., 1996).

In this paper we demonstrate that the ER-DBD dimer induces a conformation in DNA that is similar to the optimal conformation of nucleosomal DNA near the dyad. The glucocorticoid receptor (GR) DBD dimer induces such a conformation in DNA as well (Bishop and Schulten, 1994, 1996). Hence we propose that a receptor dimer and a histone octamer can achieve the most favorable interactions with nucleosomal DNA when the response element is positioned over the dyad, thus aligning the axis of symmetry of the histone octamer with that of the dimer. This positioning of the DNA on the nucleosome may facilitate the binding of other proteins involved in gene regulation.

For this purpose we have utilized molecular dynamics simulations, based on a crystallographic structure (Schwabe et al., 1993), to determine the optimal conformation of an ER-DBD dimer bound to a consensus ERE and bound to a nonconsensus ERE, ds(|AGAACA|CAG|TGACCT|). A simulation of the consensus ERE free in solution was also conducted as a control. Molecular dynamics simulations of homologous protein-DNA complexes are reported in Bishop and Schulten (1994, 1996), Eriksson et al. (1994, 1995), Eriksson and Nilsson (1995), Harris et al. (1994), and Kothekar and Kotwal (1992). Bending of DNA induced by the GR-DBD dimer was analyzed by Bishop and Schulten (1994, 1996).

In Materials and Methods we describe the molecular dynamics techniques used to simulate the three systems described above; we then define the analysis techniques. The Results section focuses on the conformational properties of the protein and DNA during our simulations that are relevant to the structure of nucleosomal DNA. In the Discussion we present experimental evidence that supports our suggested positioning of the nucleosome, and we analyze the consequences of such a positioning for the mouse mammary tumor virus promoter.

MATERIALS AND METHODS

In this section the three systems simulated and the techniques used to conduct and analyze the simulations are presented. A summary of relevant data for each simulation appears in Table 1. The sequence identity and the residue numbering for the protein and the DNA used in our simulations are presented in Fig. 3.

Structures

We utilized the crystallographic structure of the ER-DBD dimer/DNA complex (Schwabe et al., 1993) to create the systems that were simulated. The structure contains two complexes, denoted A and B, in a unit cell of the crystal. Each complex has the same positioning of the protein on the DNA, but the conformations of the proteins differ from amino acids 54–58, as labeled in Fig. 3. This segment is α-helical in both monomers of complex A and is disordered in both monomers of complex B (Schwabe et al., 1993). Each system in the present study originated from complex A.

The DNA duplex in complex A of (Schwabe et al., 1993) is 17 bp long, with a cytosine overhanging at the 5′ end of each strand. By means of molecular modeling, we paired each cytosine with a guanine and employed the resulting double-stranded DNA, ds(CC|AGGTCA|CAG|TGACCT|GG), for our simulations. This duplex is denoted ERE. The simulation referred to as er-ere contained the ER-DBD dimer, ERE, counterions, and

TABLE 1 Summary of the methods used to conduct each simulation

Simulation	ere	er-ere	er-g/ere
DNA sequence	CC|AGGTCA|CAG|TGACCT|GG		CC|AGAACA|CAG|TGACCT|GG
Protein	None	ER-DBD dimer	ER-DBD dimer
Initial coordinates	Crystal	Crystal	Modified
Total no. atoms	25,892	36,284	36,573
Total no. waters	8,218	10,944	11,040
Total no. Na^+	36	30	30
Simulation program		NAMD	
Processor (# nodes@mem.)		HP735–125 MHz (8@128 Mb)	
Energy function		All atom, CHARMM22, TIP3P (unconstrained)	
Integration method		Verlet I multiple time step with switching function	
Distance classes(Å)		(0.0–10.5), (10.5–∞)	
Time step (short/long)		1 fs/4 fs	
Coulomb evaluation		DPMTA	
Total simulation time		100 ps	
(avg. run time)/(time step)	16 s	19 s	19 s

water. The control simulation, referred to as ere, contained the naked ERE, counterions and water.

A third system was created from the same crystallographic data by mutating the first ds(GT) of ERE to ds(AA), yielding ds(CC|AG AACA|CAG|TGACCT|GG). The first half-site, i.e., ds(AGAACA), corresponds to that of a consensus glucocorticoid response element (GRE) (Martinez and Wahli, 1991), and the second half-site, i.e., ds(TGACCT), corresponds to that of a consensus ERE. This sequence is denoted by G/ERE. The simulation referred to as er-g/ere contained the ER-DBD dimer, G/ERE, counterions, and water.

Solvation

The structure of DNA is sensitive to the presence of water and ions. Hence a water bath and counterions must be included in molecular dynamics simulations (Jayaram and Beveridge, 1996). Simulations of a glucocorticoid receptor-DNA binding domain (GR-DBD) dimer/DNA complex demonstrated that nuclear hormone receptors bend DNA (Bishop and Schulten, 1994, 1996). Such bending is also observed experimentally (Nardulli and Shapiro, 1992; Petz et al., 1997; Sabbah et al., 1992). Accordingly, the solvation shells must be large enough to accommodate the conformational changes. Solvation spheres of 45 Å, 45 Å, and 39 Å radius were used in the er-ere, er-g/ere, and ere simulations, respectively. The spheres provided at least two salvation layers for the entire protein-DNA complex and several salvation layers for most of the surface of each complex.

The solvent spheres were constructed by first covering the spherical domain with a three-dimensional cubic grid and then randomly placing two hydrogens and an oxygen in each cube. A grid spacing of 3.1 Å was chosen, resulting in a density of 1.0 g/cm^3. To obtain the proper geometry for each water, the oxygens were held fixed, and 500 steps of energy minimization of the bond and angle energies were performed. All atoms were then released, and the entire system was equilibrated for 20 ps at 300K, using Berendsen temperature coupling (Berendsen et al., 1984) and a coupling constant of 0.1 ps^{-1}. At the end of the equilibration procedure an acceptable radial distribution of the atoms (see Table 2) and a stable temperature of 300K had been achieved.

To solvate the three structures, they were each centered within one of the preconstructed spheres of water. Any water molecule with an atom closer than 1.8 Å to any atom of the structure being solvated was removed. The waters that are present in the crystal structure were considered as part of the structure being solvated and maintained their positions during this procedure. Each resulting solute-solvent system was then subjected to 5 ps of molecular dynamics equilibration, during which all waters were allowed to move.

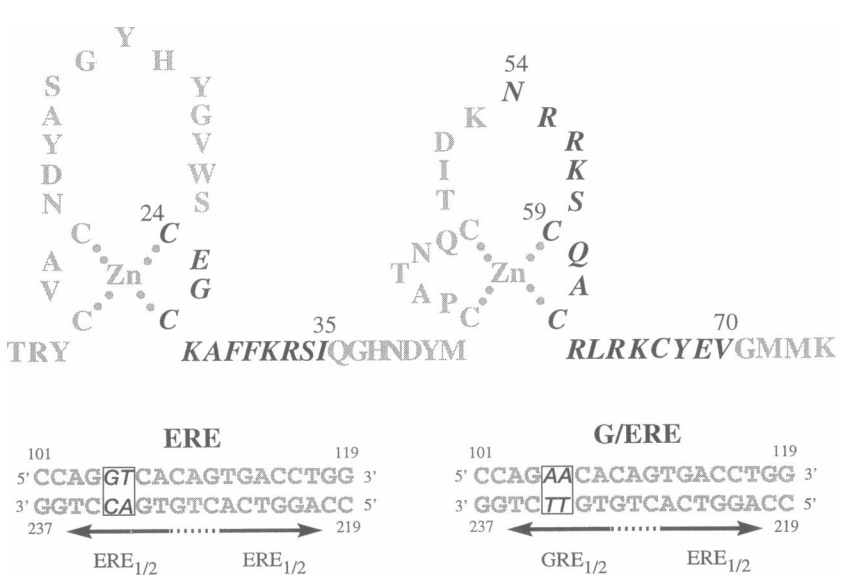

FIGURE 3 Protein (*top*) and DNA sequences (*bottom*). (*Top*) Black letters indicate the three α-helical segments of the ER-DBD, amino acids 24–35, 54–58, 59–70. Dotted lines indicate the coordination of the zinc ions. (*Bottom*) Black letters indicate the two base pairs that were mutated from the ERE contained in the crystallographic structure (Schwabe et al., 1993) to create G/ERE. Arrows and a dotted line indicate the locations of the two half-sites and the spacer of each sequence of DNA. $ERE_{1/2}$ and $GRE_{1/2}$ identify the type of half-site in each sequence.

TABLE 2 Location of peak values for the radial distribution functions and the associated coordination numbers

Property	Simulation	TIP3P
g_{OO}	2.8 Å	2.8 Å
g_{OH}	1.8 Å, 3.2 Å	1.9 Å, 3.3 Å
g_{HH}	2.5 Å, 3.7 Å	2.4 Å, 3.8 Å
$\int g_{OO} dr$	5.7	5.2
$\int g_{OH} dr$	4.0	3.9

The values in the column marked "simulation" were obtained from calculations using our equilibrated sphere of water, and the values in the column marked "TIP3P" are standard values for the constrained TIP3P water molecule (Jorgensen et al., 1983).
The integration limits for g_{OO} and g_{OH} were [0,3.5] and [0,2.5] respectively.

The number of counterions added to each system was chosen to achieve electroneutrality: 30 Na^+ ions for er-ere and er-g/ere and 36 Na^+ ions for ere. To determine the initial location of the Na^+ ions for a given structure, every water molecule located farther away than 5 Å from the protein-DNA complex was considered a possible location for an ion. The electrostatic potential was calculated for the oxygen of each water molecule considered, and the water molecules were ranked according to this potential, i.e., the water with the highest electrostatic potential associated with its oxygen was ranked highest, etc. In an iterative procedure, 30 water molecules (36 in case of ere) were replaced with Na^+ ions. During each iteration the electrostatic potential was recalculated, the highest ranked water molecule was replaced with an ion, and all water molecules within 9 Å of the ion were removed from consideration in subsequent iterations.

Molecular dynamics simulations

All simulations were performed on a cluster of workstations using the molecular dynamics program NAMD (Nelson et al., 1996) and version 22 (MacKerell et al., 1995; Mackerell et al., submitted for publication) of the CHARMM (Brooks et al., 1983) force field. Additional parameters for the tetrahedral coordination of the zinc ions to cysteine residues were the same as those used by Eriksson et al. (1995). NAMD provides the option of calculating full electrostatic interactions through the use of a fast multipole expansion algorithm, namely the program DPMTA (Rankin and Board, 1995). This option was used throughout each simulation to calculate electrostatic interactions between atoms beyond a cut-off distance of 10.5 Å to a relative accuracy of 10^{-6}.

In NAMD the frequency of evaluating the long-range electrostatic interactions is reduced through the use of a Verlet I two-time step algorithm (Biesiadecki and Skeel, 1993; Grubmüller et al., 1991). The two-time step scheme implemented in NAMD relies on the separation of the electrostatic interactions into two distance classes according to the distance between the interacting atoms (Grubmüller et al., 1991).

Test simulations of the solvated ER-DBD dimer/DNA system demonstrated that a 1-fs short time step and a 4-fs long time step conserved the total energy to within 0.006% for each picosecond of simulation. Utilizing these two time steps provided a speed-up by a factor of 3.7 compared to a conventional single time step simulation with a 1-fs time step. Time steps of 1 fs and 4 fs were chosen for all subsequent simulations.

The total energy diverged if the long time step was longer than 4 fs. We found that the total energy diverged more slowly when we used two-time steps of 1 fs and 6 fs rather than using two-time steps of 1 fs and 5 fs, indicating a resonance between 4 fs and 6 fs. The lack of energy conservation manifested itself through the bonded energy, suggesting that the resonance is due to a normal mode vibration involving the OH bond, which for the CHARMM force field occurs at approximately 3700 cm^{-1} (9 fs) (Watanabe and Karplus, 1993). The excitation of resonances was suggested earlier (Grubmüller et al., 1991) and has since been investigated (Biesiadecki and Skeel, 1993; Bishop et al., submitted for publication) for multiple time step methods. The resonance between 4 fs and 6 fs places an upper limit on the long time step that can be used for simulating systems with unconstrained OH vibrations.

The following protocol was employed for each simulation. An initial velocity distribution, corresponding to 300 K, was assigned to the system, and 5 ps of molecular dynamics equilibration, with coupling to a temperature bath of 300 K, was conducted. Because the solvent had previously been equilibrated to 300K during a 20 ps simulation, 5 ps of additional equilibration was sufficient to provide a uniform temperature distribution throughout the solute-solvent system. After equilibration, 100 ps of molecular dynamics was completed for each system, using the parameters listed in Table 1.

STRUCTURE ANALYSIS

The conformation of DNA in each simulation was analyzed by evaluating the inter-base-pair parameters of roll (ρ), tilt (τ), and twist (Ω). These parameters were extracted from each trajectory at an interval of 1 ps with the Molecular Dynamics Analysis Toolchest (Ravishanker et al., 1989; Sklenar et al., 1989).

The helix repeat

$$\Phi = \frac{N \times 360^\circ}{\sum_{i=1}^{N} \Omega_i} \tag{1}$$

was calculated for each snapshot of the three trajectories. Here, $\Sigma_{i=1}^{N} \Omega_i$ represents the total inter-base-pair twist for each response element. N is the number of base-pair steps and is equal to 14 for each response element. The two base pairs at the termini of each DNA segment, ds(GG) and ds(CC), were not included in this analysis.

Bending of the DNA was measured by combining the values of roll, ρ_i, and tilt, τ_i, to estimate the bend, β_i, at each base-pair step, i. The bend was approximated as

$$\beta_i = \sqrt{(\rho_i^2 + \tau_i^2)}. \tag{2}$$

The angle

$$\beta_T = \frac{\sum_{ix=1}^{N} \beta_i}{N} \tag{3}$$

is a measure of the deviation per base step from a linear conformation, defined by $\beta_T \equiv 0$, for a given snapshot of a trajectory; β_T does not provide any information about the direction of bending. The sum in Eq. 3 extended over the same 14-bp steps as for the calculations of helix repeat. To evaluate the deformations that create bending, scatter plots of ρ_i versus τ_i were analyzed.

To measure a directed bend of DNA during each simulation, a line segment was fit by least squares to each of the half-site axes, as determined by the Molecular Dynamics Analysis Toolchest (Ravishanker et al., 1989; Sklenar et al., 1989), and the angle between the two line segments, denoted $\alpha_{h,h}$, was determined. This measure disregards local bending of the half-sites. A similar method was used to measure global motions of the ER-DBD monomers relative to each other. For this purpose, a line segment was fit by least squares to the backbone of the reading helices, amino acids Glu-25 through Ser-34 in Fig. 3, and the angle be-

tween these two line segments, denoted $\alpha_{r,r}$, was determined. Subscripts will be used to indicate standard deviations when we report values for the above quantities, e.g., $\alpha_{r,r} = 180^{\circ}_{10}$ indicates an average value of 180° with a standard deviation of 10°.

CORRELATION OF DATA

To determine if a correlation between two data sets existed, the covariance,

$$r = \frac{\sum_t (X_t - \bar{X})(Y_t - \bar{Y})}{[\sum_t (X_t - \bar{X})^2 \sum_t (Y_t - \bar{Y})^2]^{1/2}}, \quad (4)$$

was calculated. Here X_t are the data values obtained from each 100-ps trajectory at 1 ps intervals, and $\bar{X}$ is the average value of X_t over the trajectory.

RESULTS

First, analysis of the simulations in terms of the root mean square (rms) difference from the initial structure has been carried out for each system. The results are presented in Fig. 4. The rms values for simulation ere indicate that a stable conformation has not been achieved after 100 ps. It is known that simulations of naked DNA typically require longer simulation times to achieve a stable conformation (Cheatham and Kollman, 1996; McConnell et al., 1994; Yang and Pettitt, 1996). Convergence to a stable conformation in simulation ere is further hindered by the fact that the initial DNA conformation stemmed from a complex with a protein. In contrast, simulations er-ere and er-g/ere achieved stable DNA configurations after about 50 ps, indicating that the protein stabilizes the conformation of the DNA. Accordingly, we focus further analysis on the properties of the protein and DNA that are relevant to the structure of nucleosomal DNA and on the conformation of the DNA in complex with the dimer. Below we evaluate the helix repeat, the relative orientation of the monomers, and bending of the DNA.

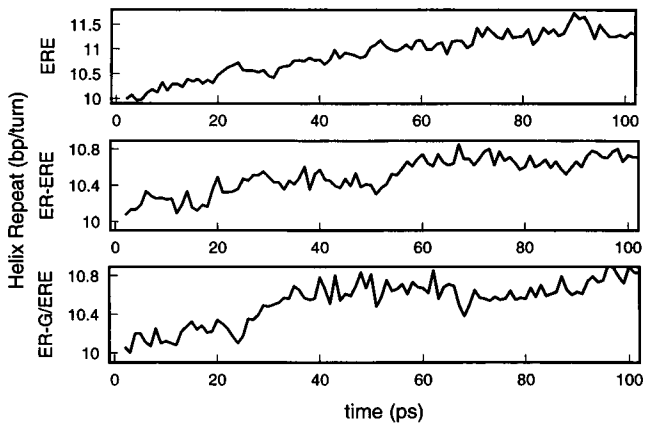

FIGURE 5 Helix repeat. The helix repeat of DNA during simulation ere exceeded the expected solution value of 10.5 bp/turn (*top*). The helix repeat of the DNA during simulations er-ere (*middle*) and er-g/ere (*bottom*) stabilized at 10.7 bp/turn.

Helix repeat

Helix repeat values were determined according to Eq. 1 and are presented for the duration of each simulation in Fig. 5. The helix repeat in the crystallographic structure is 10.0 bp/turn (Schwabe et al., 1993). During simulations er-ere and er-g/ere, the helix repeat increased to 10.7 bp/turn and remained constant, indicating that a stable protein-DNA complex has been achieved. The helix repeat during simulation ere eventually exceeded 11.0 bp/turn, indicating an underwound conformation of the DNA. The unwinding of the naked DNA during simulation ere beyond the observed solution value of 10.5 bp/turn (Klug and Rhodes, 1980) is expected because DNA typically becomes underwound in rather different molecular dynamics simulations (Levitt, 1982; Cheatham and Kollman, 1996; Yang and Pettitt, 1996).

A change in helix repeat from 10.0 to 10.7 bp/turn requires approximately 30° of unwinding of the response element. In this respect we note that a maximum difference of about 20° in $\alpha_{r,r}$ the angle between monomers was found

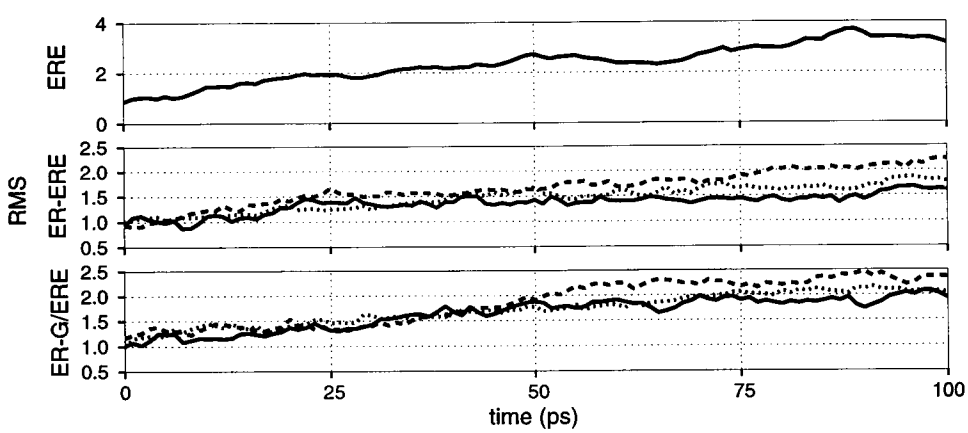

FIGURE 4 The root mean square difference of all heavy atoms from the initial structure for simulations ere (*top*), er-ere (*middle*), and er-g/ere (*bottom*). The solid line represents the rms difference for the DNA, the dashed line represents the rms difference for monomer 1, and the dotted line represents the rms difference for monomer 2. The heavy atoms of each molecular component were fit by least squares (Kabsch, 1976) to the initial structure before determination of the rms.

to occur during our simulations as indicated in Fig. 7. Below we demonstrate that changes in $\alpha_{r,r}$ are correlated to the net twist of the spacer and that changes in twist of the half-sites require a change in the protein-DNA interface, which is not measured by changes in $\alpha_{r,r}$.

Twist

Twist measures the rotation about the DNA helical axis between base pairs. Average values of twist are presented in Fig. 6. For segments of DNA where the bases are in contact with the dimer, e.g. the half-sites, optimal interactions between the bases and the dimer require specific values of twist. For segments of DNA where the bases are not in contact with the dimer, e.g., the spacer region or free DNA, the range of twist values is determined by the DNA sequence.

In the crystallographic structure the twist values corresponding to the half-sites are similar at equal sequence distances from the center of the response element (Schwabe et al., 1993), reflecting the dyad symmetry of the protein-DNA complex. Unwinding of the DNA from the initial crystallographic conformation, described above by changes in helix repeat, can be discerned for individual base-pair steps in Fig. 6.

In simulation ere there are no external factors that limit the conformation of the DNA; hence the DNA was freer to unwind in this simulation than in the case of simulations er-ere or er-g/ere, e.g., ds(AG) of the first half-site achieved a twist of $24.6^{\circ}_{8.1}$, which is 10° less than the initial twist of 34.9° (Schwabe et al., 1993).

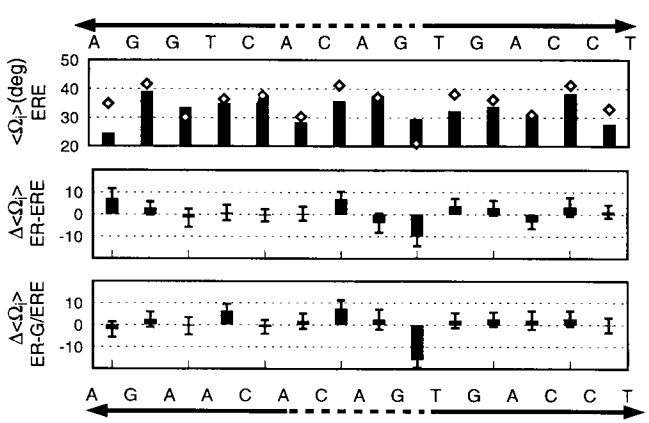

FIGURE 6 Average and relative twist values. The average twist, $\langle\Omega_i\rangle$, at each base-pair step, i, during simulation ere is plotted as a bar graph (*top*). Diamonds indicate values from the crystallographic structure (Schwabe et al., 1993). Relative twist values obtained from simulations er-ere (*middle*) and er-g/ere (*bottom*) are plotted as differences from the crystallographic values, $\Delta\langle\Omega_i\rangle$; error bars denote the standard deviation. Positive values of $\Delta\langle\Omega_i\rangle$ represent unwinding with respect to the initial crystallographic conformation. ERE and G/ERE sequences are shown at the top and bottom of the figure, respectively. For each sequence of DNA arrows indicate the two half-sites, and dotted lines indicate the spacer.

With the exception of the first ds(AG) in simulation er-ere and the first ds(AC) in simulation er-g/ere, unwinding of the half-sites is less than 5° for any given step in the protein-DNA complexes. During simulation er-ere the change in twist for ds(AG) from 34.9° in the crystallographic structure (Schwabe et al., 1993) to $27.6^{\circ}_{4.4}$ coincided with the formation of a water bridge between the adenosine and Lys-28 that was not observed in the crystallographic structure. During simulation er-g/ere, the change in twist for the first ds(AC) from 36.5° in the crystallographic structure (Schwabe et al., 1993) to $30.1^{\circ}_{1.1}$ resulted from the mutation of two base pairs and from the addition of water to the protein-DNA interface compared to a consensus half-site. We conclude that a significant change in the average twist for a half-site accompanies changes in the protein-DNA interface. A thorough analysis of the interactions at the protein-DNA interface is discussed elsewhere (Kosztin et al., manuscript in preparation).

No direct contacts existed between the dimer and the bases of the spacer. Hence twist values for the spacer exhibited the greatest deviation from the initial crystallographic structure. In particular, ds(GT) exhibited an average twist of $31.0^{\circ}_{4.4}$ in simulation er-ere and of $36.7^{\circ}_{3.6}$ in er-g/ere. These values are greater than the initial value of 21.0° reported by Schwabe et al. (1993) and are closer to the ideal value of $35.8^{\circ}_{4.4}$ for ds(GT) reported by Gorin et al. (1995).

Although individual values of twist describing the spacer did not appear to be constrained by interactions with the dimer, the net twist of the spacer region, Ω_{spacer}, was affected by the dimer, as demonstrated below.

Relative orientation of monomers

The relative orientation of the monomers, measured by $\alpha_{r,r}$, correlates with Ω_{spacer}, defined as $\Sigma_i\ \Omega_i$ for ds(ACAGT) (see Fig. 7). The covariance of Ω_{spacer} and $\alpha_{r,r}$ was 0.69 in simulation er-ere and 0.55 in er-g/ere, indicating a signifi-

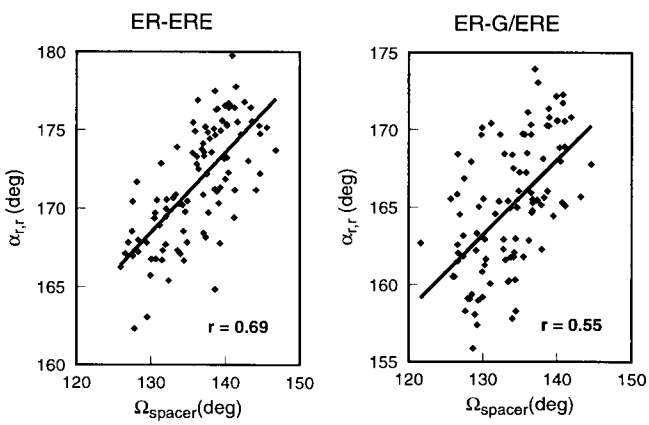

FIGURE 7 Twist versus monomer orientation. The twist of the spacer, Ω_{spacer}, is plotted versus the angle between monomers, $\alpha_{r,r}$, for snapshots of simulations er-ere (*left*) and er-g/ere (*right*) taken at intervals of 1 ps. Lines indicate a least-squares fit to the data. The covariance is indicated by *r* in each graph.

cant correlation between unwinding of the spacer region and the relative orientation of monomers.

In the crystallographic structure (Schwabe et al., 1993), the net twist of the spacer is 137° and the two reading helix axes are nearly antiparallel, $\alpha_{r,r}$ = 172°, lying in a plane tangent to a cylindrical surface that encloses the DNA. Changes in $\alpha_{r,r}$ measure both a rotation of the monomers about the DNA helical axis, i.e., the skewness of the axes, and deviations of the axes from their initial antiparallel orientation within the tangent plane. The underlying motion represents a relaxation from the constraints imposed on the complex by crystal packing, and the correlation between Ω_{spacer} and $\alpha_{r,r}$ indicates that the spacer serves to maintain an optimal alignment of each half-site with the respective monomer during the relaxation.

Bends

Net bends

To determine whether there was a directed bend in the DNA, the angle $\alpha_{h,h}$ between half-sites was determined. The value of $\alpha_{h,h}$ obtained from our analysis of the crystallographic structure is 15°. The average values of $\alpha_{h,h}$ for our simulations, presented in Table 3, are higher. The crystallographic analysis did not report the DNA as having a bend (Schwabe et al., 1995).

We suggest that $\alpha_{h,h}$ approximates the bend measured in electrophoretic mobility shift experiments (Nardulli and Shapiro, 1992; Petz et al., 1997; Sabbah et al., 1992). We emphasize that $\alpha_{h,h}$ is an approximate measure which assumes that the half-sites are linear and that the bending occurs in the spacer region. It does not accurately describe the local conformation of the DNA. Experimental and theoretical values for the bending of DNA induced by the ER-DBD and GR-DBD dimers are also presented in Table 3.

The total bending, β_T, of the DNA was calculated using roll, ρ_i, and tilt, τ_i, according to Eq. 3. This measure is sensitive to differences in the conformation of DNA but does not measure a directed bend, as does $\alpha_{h,h}$. The crystallographic structure of the GR-DBD dimer/DNA complex (Luisi et al., 1991) and the ER-DBD dimer/DNA complex (Schwabe et al., 1995) both have a value of β_T of 8°. The average value of β_T for each simulation is listed in Table 3 and indicates that the DNA was significantly less bent in the original crystal structures than in our current simulations of ER-DBD dimer/DNA complexes or in our previous simulations of GR-DBD dimer/DNA complexes (Bishop and Schulten, 1996). The increased bending of the DNA as indicated by $\langle\beta_T\rangle$ agrees with an increase in $\alpha_{h,h}$ and the appearance of additional bends located in the half-sites, as described below.

The values of bending obtained for the simulations of the GR-DBD dimer/DNA complexes (Bishop and Schulten, 1996) are higher than the values obtained in the current simulations of the ER-DBD dimer/DNA complexes. In this regard, we note that the simulations reported by Bishop and Schulte (1996) did not include counterions, whereas the systems in the present simulations are completely neutralized by counterions. We have found that the presence of counterions in a simulation of a protein-DNA complex significantly weakens the electrostatic interactions between positively charged amino acids and the phosphate groups of DNA, thus decreasing the ability of the protein to induce conformational changes in DNA. It is known that ion concentration can also significantly affect protein-DNA interactions in vivo (Record et al., 1976).

TABLE 3 Bending of DNA

Simulation	$\langle\beta_T\rangle$	$\langle\alpha_{h,h}\rangle$	Experiment
ere	14°_{2}	22°_{6}	NA
er-ere	12°_{2}	19°_{4}	34° (Nardulli and Shapiro, 1992)
er-g/ere	13°_{2}	19°_{4}	NA
gre	15°_{3}	NA	NA
gr-gre$_3$	17°_{2}	$35^{\circ\#}$	28° (Petz et al., 1997)
gr-gre$_4$	18°_{3}	$35^{\circ\#}$	NA

The values for the GR-DBD dimer/DNA complexes were obtained from the simulations reported by (Bishop and Schulten (1996). Experimental data were taken from the stated references. Subscripts denote the standard deviation; NA indicates that data were not available.

#As reported by Bishop and Schulten (1996), indicating a final value and not an average.

Individual bends

To analyze the local structure of the DNA, the average bend values, $\langle\beta_i\rangle$, were measured; they are presented in Fig. 8 for each simulation. Optimal contacts between the monomers and the half-sites require a specific geometry of the DNA, and accordingly, bends in the half-sites are induced by

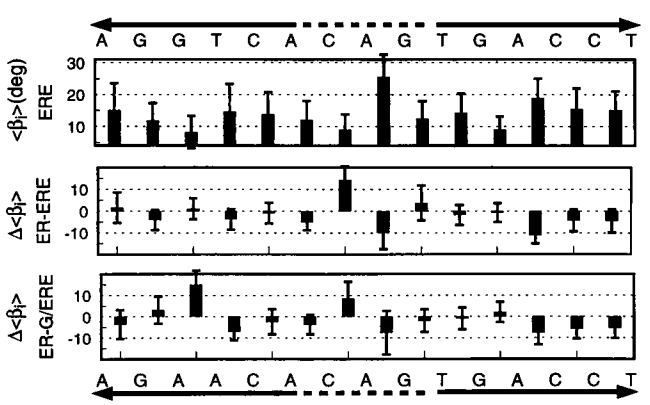

FIGURE 8 Average bend values. The average bend, $\langle\beta_i\rangle$, during simulation ere (*top*) is plotted for each base pair. The average bend at each step during simulations er-ere (*middle*) and er-g/ere (*bottom*) are plotted as differences, $\Delta\langle\beta_i\rangle$, from the corresponding values in ere. Error bars denote a standard deviation. Positive values of $\Delta\langle\beta_i\rangle$ indicate greater bending; negative values indicate less bending. ERE and G/ERE sequences are printed at the top and bottom of the figure, respectively. For each sequence of DNA, arrows indicate the two half-sites, and dotted lines indicate the spacer.

interactions with the respective monomers. At the site of the mutations in G/ERE, i.e., ds(AA), the degree of bending differed by more than 10° from the corresponding site in er-ere. In this region, the twist was also found to differ between simulations, as noted above.

However, the spatial extent of the conformational differences that can develop between the mutated and unmutated half-sites is limited by interactions between the protein and phosphate groups of the DNA. These interactions define "checkpoints" through which the DNA helical axis must pass and involve the two phosphate groups at the 5′ end of each strand of each half-site, i.e., four phosphate groups for each half-site. These protein-DNA interactions are highly conserved throughout the family of hormone receptor/DNA complexes (Schwabe et al., 1993; Gewirth and Sigler, 1995). Thus, although the mutations introduced into the system altered the protein-DNA interface as well as the local structure of the DNA, the global structure of the DNA in the er-ere and er-g/ere simulations remained similar. The ability of the ER-DBD dimer to bind to and induce a conformation in G/ERE that is similar to the conformation of ERE is to be expected, because the G/ERE is a functional response element (Schwabe et al., 1995).

The spacer, which is located between "checkpoints" of the first and second half-sites but does not have any specific contacts with the dimer itself, serves to align each half-site for optimal interactions with the protein. In this manner, the spacer effectively isolated the unmutated half-site in er-g/ere from the conformational changes in the mutated half-site, as evidenced by the similarity in conformation of the second half-site in simulation er-g/ere to that in simulation er-ere.

The high degree of bending during simulation ere, as indicated by $\langle \beta_T \rangle$ in Table 3, was partially due to a significant bend of the central base-pair step ds(AG). The average bend at this step was $25.6^{\circ}_{7.0}$ (Fig. 8). Such a large bend could arise because the conformation of the naked DNA was not restricted by the dimer.

Snapshots of the bends

Overall bends in the DNA during simulations er-ere and er-g/ere are described by projections onto two perpendicular planes. The two projections are represented in Fig. 9 for a snapshot taken from simulation er-ere. In the so-called vertical plane, the bend is localized near the spacer and is oriented such that the dimer is on the convex surface of the bend. The bend is toward the major groove.

In the so-called horizontal plane two bends arose. The two bends are oriented so that they cancel each other and create an S-shaped bend in the DNA axis. A similar conformation of the helical axis was observed in simulations of GR-DBD dimer/DNA complexes (Bishop and Schulten, 1996). The S-shape is a consequence of the dyad symmetry of the dimer/DNA complexes.

We note that intact receptors induce a bend in the response element ranging from 60° to 70°, compared to the bend of approximately 30° induced by the DBD (Bishop and Schulten, 1996; Nardulli and Shapiro, 1992; Petz et al., 1997; Sabbah et al., 1992). The extent of the bend is limited to the 15 bp that constitute a response element, so that the average bend per base pair is approximately 4.3°. This bending, if confined to the so-called vertical plane, is the degree of bending necessary to uniformly bend DNA to match the surface of a histone,

$$\frac{1.75 \text{ turns}}{\text{nucleosome}} \times \frac{360^{\circ}}{\text{turn}} \times \frac{1 \text{ nucleosome}}{146 \text{ bp}}. \qquad (5)$$

Bending in the horizontal plane will increase the average bend per base pair and is expected to result in an S-shaped bend of the DNA, similar to the one arising in our simulations.

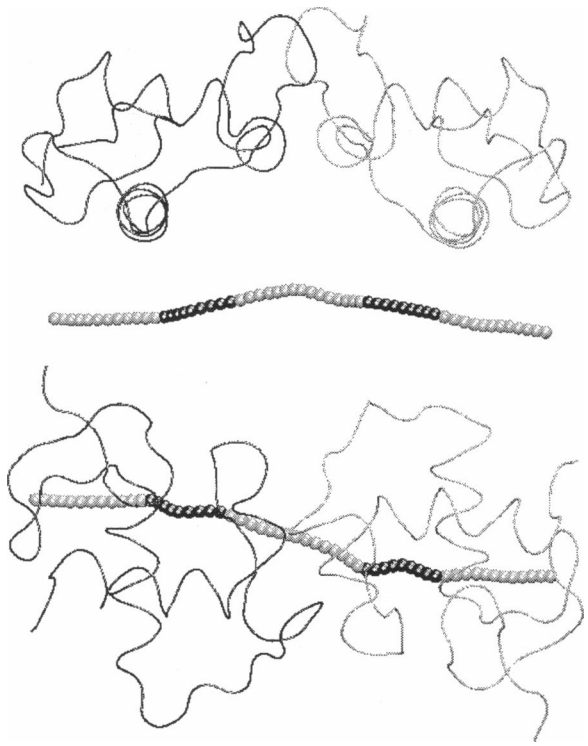

FIGURE 9 Orthogonal projections of a snapshot taken from simulation er-ere. The dimer is represented by a grey string that traces the backbone of each monomer. The DNA is represented as beads on a string. Black beads correspond to ds(TCA) and ds(TGA). The bend in a projection onto a vertical plane is confined to the spacer between the black beads (*top*). Bends in a projection onto a horizontal plane are localized near ds(TCA) and ds(TGA) and are oriented so as to create an S-shaped bend.

Scatter plots of roll and tilt

The bends described above are due to the roll and tilt between base pairs plotted in Fig. 10. These plots represent the conformation of DNA in snapshots taken from each trajectory. By definition, the roll of a base-pair step, ds(XY), on the Watson strand of duplex DNA is identical to the roll of the same step on the Crick strand, ds(Y′X′), and

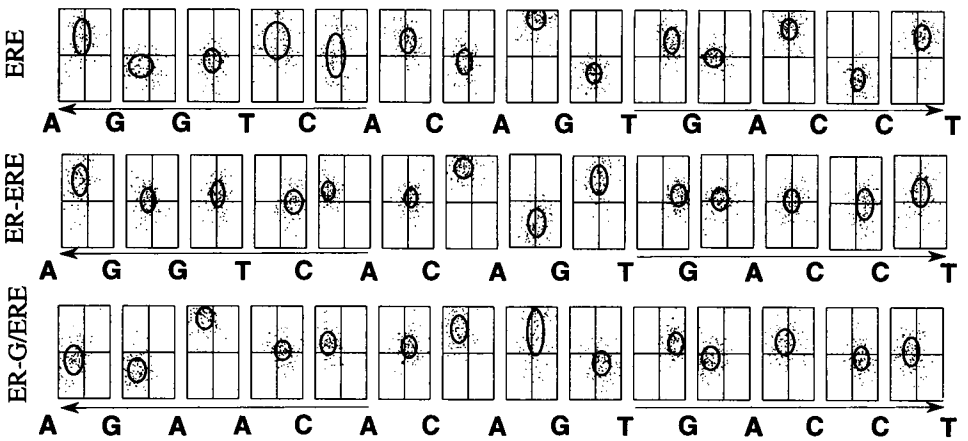

FIGURE 10 Scatter plots of tilt and roll. Simulations ere (*top*), er-ere (*middle*), and er-g/ere (*bottom*) are represented by scatter plots of data obtained from snapshots of each trajectory taken at intervals of 1 ps. Tilt is plotted on the horizontal axis; each plot has a range [−15°, +15°]. Roll is plotted on the vertical axis; each plot has a range [−30°, +30°]. The center of each ellipse indicates the average value of tilt and roll, and the horizontal and vertical extents of each ellipse indicate the standard deviation of tilt and roll, respectively.

the tilt for ds(XY) is opposite the tilt for ds(Y′X′). Hence, symmetrical bending is reflected in these plots by identical roll and opposite tilt values at base-pair steps that are equidistant from the central ds(A).

From Fig. 10 one can discern that, for simulations er-ere and er-g/ere, bends in the spacer were primarily due to roll, whereas bends in the half-sites were due to a combination of roll and tilt. The highest average tilt observed in simulation er-ere corresponded to ds(TCA) and ds(TGA) of the first and second half-sites, respectively. During simulation er-g/ere, similarly high values of tilt were observed for the corresponding trinucleotides ds(ACA) and ds(TGA). The trinucleotide ds(TGA), which is equivalent to ds(TCA), has the highest bending propensity of all possible trinucleotides (Brukner and Sánchez, 1995).

The above trinucleotides are adjacent to the spacer and were separated by an average twist, $\langle\Omega_{spacer}\rangle$, of 136°_{5} during simulation er-ere and of 134°_{5} during er-g/ere. When the path of the major groove is traced from the center of the response element toward one of these trinucleotides, it rotates by approximately 135°/2 about the DNA axis from its direction opposite the dimer at the center of the response element. As this path continues over the trinucleotides of interest, it passes through a horizontal plane and becomes directed toward the dimer again, as can be determined by visually tracing the path of the major groove in Fig. 2. Bending of the two trinucleotides by symmetrical roll and tilt creates an S-shape in the DNA axis when projected onto a horizontal plane, as represented in Fig. 10.

We note here that for a consensus GRE, the trinucleotides adjacent to the spacer are ds(ACA) and ds(TGT), which have either ds(CA) or ds(TG) in common with an ERE. The dinucleotide ds(CA), which is equivalent to ds(TG), possesses a multiplicity of allowed roll and tilt states (Gorin et al., 1995). Thus a consensus GRE or ERE allows a multiplicity of conformations at sites that can create the S-shape in the DNA helical axis described above; the ability to achieve this S-shape is an intrinsic property of a consensus response element.

The bending propensity of DNA is known to be anisotropic; analysis of crystallographic data bases indicates that the ratio of roll to tilt is approximately 2:1 (Olson, 1996; Young et al., 1995). This anisotropy appears in our scatter plots as the ratio of the lengths of the vertical to horizontal axes of each ellipse. The extents of the vertical and horizontal axes of each ellipse represent the standard deviation of the roll and tilt, respectively. The ratio is approximately 1.75 for each simulation; actual values are listed in Table 4. This ratio is unaffected by differences in the absolute conformation of the DNA indicated by $\langle|\text{Roll}|\rangle/\langle|\text{Tilt}|\rangle$ in Table 4.

DISCUSSION

Our simulations of an ER-DBD dimer complexed with different DNA sequences revealed conformational changes from the crystallographic structure (Schwabe et al., 1993) that was used to initiate the simulations. We found that a helix repeat of 10.7 bp/turn was energetically more favorable for the dimer/DNA complexes than the helix repeat of 10.0 bp/turn in the crystallographic structure. The dimer was also found to induce a bend in the DNA helical axis when projected onto one plane and an S-shaped bend when projected onto an orthogonal plane (see Fig. 9). Our simulation of free DNA produced a bent and underwound but not symmetrical conformation. We conclude that the conformation of DNA bound to an ER-DBD dimer reflects the dyad symmetry of the dimer.

A similar conformation of DNA was observed during simulations of GR-DBD dimer/DNA complexes (Bishop and Schulten, 1996). We suggest that the conformation represents an energetically optimal conformation for a hormone receptor dimer/DNA complex and that the particular conformation induced in the DNA has a functional role in

TABLE 4 Roll and tilt statistics

Simulation	$\langle\|\text{Roll}\|\rangle/\langle\|\text{Tilt}\|\rangle$	$\langle\sigma_{\text{Roll}}\rangle/\langle\sigma_{\text{Tilt}}\rangle$
ere	9.9° /2.7°	8.4° /5.0°
er-ere	6.7° /3.7°	7.9° /4.5°
er-g/ere	7.7° /5.0°	8.3° /4.8°

the hormone response mechanism (Beato et al., 1996a; Truss et al., 1995).

For nucleosomal DNA, a similar S-shaped bend and helix repeat are observed near the nucleosome's axis of dyad symmetry (Richmond et al., 1984; Hayes et al., 1990; Puhl and Behe, 1993). Optimal protein-DNA interactions between a histone octamer and DNA, as well as between a hormone receptor dimer and DNA, can be achieved simultaneously if the hormone receptor dimer/DNA complex is positioned over the nucleosome dyad. This positioning also satisfies the preferred rotational phasing of nucleosomal DNA, i.e., the minor groove faces away from the histone octamer at the dyad (Richmond et al., 1984) and hence toward the dimer.

In this regard we note that nucleosome positioning can be achieved in vitro by means of DNA with intrinsically flexible or intrinsically bent sequences. Such positioning is most effective when the sequence possessing the intrinsic properties is designed to be positioned near the nucleosome dyad (Travers, 1987).

The question remains whether positioning can be induced by hormone receptor binding and whether it might serve a biological function. Much effort has recently been devoted to measuring the degree to which nucleosomal DNA is free or fixed in terms of its position on the histone octamer (Beato et al., 1996a; Polach and Widom, 1995). An interesting example is furnished by the mouse mammary tumor virus (MMTV) promoter. The MMTV promoter consists of six nucleosomes (Richard-Foy and Hager, 1987) that regulate gene expression by GRs. The nucleosome adjacent to the nucleosome containing the TATA box is referred to as nucleosome B. Nucleosome B contains four GRES, one of which is a near-perfect GRE, GRE_p. In vitro measurements of the positioning of DNA on nucleosome B indicate that only two of the four GREs are accessible to GR binding before the GR binds; one of these two GREs is GRE_p (Piña et al., 1990). This positioning is indicated in Fig. 11.

Nucleosome B has been reported to occupy as many as five distinct positional frames spanning a length of approximately 50 bp (Fragoso et al., 1995; Roberts et al., 1995). This variability allows GRE_p to be positioned over the nucleosome dyad. Such a positioning would be energetically favorable once GR binds, because the helix repeat, bending, and symmetry of the conformation of GRE_p in complex with a hormone receptor dimer are similar to the conformation of nucleosomal DNA near the dyad. It was noted by Truss et al. (1995) that the base pairs near the dyad of nucleosome B were protected by the footprint of a bound receptor, indicating that, in fact, such a positioning of the receptor on the nucleosome is achieved. Binding of GR to a position over the dyad might interfere with the binding of linker histone, which also binds near the nucleosome dyad. And in fact, the binding of GR to nucleosome B leads to a displacement of linker histone (Bresnick et al., 1992).

The binding of a GR dimer may not necessarily fix this positioning, but rather it may alter the frequency of occupation of each of the multiple frames observed by Fragoso et al. (1995) and Roberts et al. (1995). However, no change in the frequency of occupation of each frame or in the positioning of DNA on nucleosome B was detected upon the introduction of GR to systems containing constructs of nucleosome B (Fragoso et al., 1995; Roberts et al., 1995; Truss et al., 1995). It was noted that such measurements may not be resolved by the experimental techniques employed (Fragoso et al., 1995).

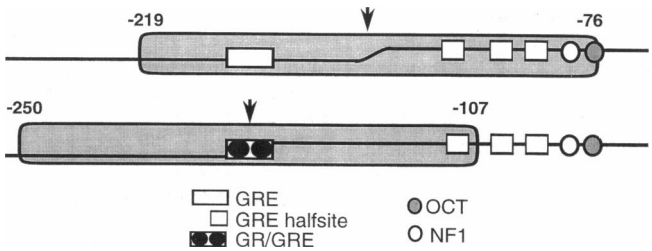

FIGURE 11 Rearrangement of nucleosome B in the mouse mammary tumor virus promoter. The positional frame of nucleosome B is indicated by a grey box and the position of the dyadic axis by an arrow. (*Top*) Initial positioning frame with GRE off the dyadic axis; two GRE half-sites and OCT, NF1 binding sites are blocked (Perlmann and Wrange, 1988). (*Bottom*) Binding of GR shifts the positioned frame of nucleosome B, moving GRE to the dyadic axis. Two GREs and binding sites for OCT, NF1 become exposed.

The result of an increased occupancy of the positional frame that locates the GRE_p over the nucleosome dyad increases the accessibility of other segments of DNA for protein binding. A shift to this positional frame translates two of the GREs and two other sites, OCT and NF1, out of the region of contact with the histone octamer, as indicated in Fig. 11. Binding of GR would thus increase the frequency of exposure of these binding sites, and thus the accessibility to DNA-binding proteins. The shift, therefore, agrees with the observation that all four GREs are occupied in vivo (Truss et al., 1995) and that the binding of protein to OCT and NF1 first requires binding of GR to the nucleosome (Archer et al., 1992).

The tripartite structure of the histone octamer (Arents et al., 1991) possesses other symmetries that might provide alternative sites for the localization of symmetrical protein-DNA complexes, but no unique structural features of nucleosomal DNA have been observed for these regions for a stable nucleosome. Such features might be achieved if the interface between the (H2A-H2B) dimer and the $(H3\text{-}H4)_2$ tetramer in a histone octamer were altered. Changes in the histone octamer complex are realizable because the dimer is known to readily dissociate from the tetramer (Eickbrusch and Moudrianakis, 1978).

We thank J. Schwabe for making the crystallographic structure of the estrogen receptor DNA binding domain dimer/DNA complex available to us (Schwabe et al., 1993) and R. Skeel, M. Nelson, R. Brunner, and A. Gursoy for help with NAMD. We also thank the Beckman Institute for Advanced Science and Technology.

This work was supported by grants from the National Institutes of Health (PHS 5 P41 RRO5969-04), the National Science Foundation (BIR-9318159 BiR 96-23827 EQ), and the Roy J. Carver Charitable Trust.

REFERENCES

Archer, T. K., P. Lefebvre, R. G. Wolford, and G. L. Hager. 1992. Transcription factor loading on the MMTV promoter: a bimodal mechanism for promoter activation. *Science,* 20115:1573–1576.

Arents, G., R. W. Burlingame, B.-C. Wang, W. E. Love, and E. N. Moudrianakis. 1991. The nucleosomal core histone octamer at 3.1 Å resolution: a tripartite protein assembly and a left-handed superhelix. *Proc. Natl. Acad. Sci. USA.* 88:10148–10152.

Beato, M., R. Candau, S. Chávez, C. Möws, and M. Truss. 1996a. Interaction of steroid hormone receptors with transcription factors involves chromatin remodelling. *J. Steroid Biochem. Mol. Biol.* 56:47–59.

Beato, M., S. Chávez, and M. Truss. 1996b. Transcriptional regulation by steroid hormones. *Steroids.* 61:240–251.

Beato, M., P. Herrlich, and G. Schütz. 1995. Steroid hormone receptors: many actors in search of a plot. *Cell.* 83:851–857.

Berendsen, H. J. C., J. P. M. Postma, W. F. van Gunsteren, A. DiNola, and J. R. Haak. 1984. Coupling to a heat bath. *J. Chem. Phys.* 81:3684–3688.

Biesiadecki, J. J., and R. D. Skeel. 1993. Danger of multiple-time-step methods. *J. Comput. Phys.* 109:318–328.

Bishop, T., and K. Schulten. 1994. Molecular dynamics study of a sequence specific protein-DNA interaction. *In* Computational Approaches in Supramolecular Chemistry, G. Wipff, editor. Kluwer Academic Publishers, Boston. 419–439.

Bishop, T., and K. Schulten. 1996. Molecular dynamics study of glucocorticoid receptor-DNA binding. *Proteins Struct. Funct. Genet.* 24: 115–133.

Bresnick, E. H., M. Bustin, V. Marsaud, H. Richard-Foy, and G. L. Hager. 1992. The transcriptionally-active MMTV promoter is depleted of histone H1. *Nucleic Acids Res.* 20:273–278.

Brooks, B. R., R. E. Bruccoleri, B. D. Olafson, D. J. States, S. Swaminathan, and M. Karplus. 1983. CHARMm: a program for macromolecular energy, minimization, and dynamics calculations. *J. Comput. Chem.* 4:187–217.

Brukner, I., and R. Sánchez. 1995. Sequence-dependent bending propensity of DNA as revealed by DNase I: parameters for trinucleotides. *EMBO J.* 14:1812–1818.

Cheatham, T. E., and P. A. Kollman. 1996. Observation of the A-DNA to B-DNA transition during unrestrained molecular dynamics in aqueous solution. *J. Mol. Biol.* 259:434–444.

Eickbrusch, T. H., and E. N. Moudrianakis. 1978. The histone core complex: an octamer assembled by two sets of protein-protein interactions. *Biochemistry.* 17:4955–4963.

Eriksson, M., T. Härd, and L. Nilsson. 1994. Molecular dynamics simulation of a DNA binding protein free and in complex with DNA. *In* Computational Approaches in Supramolecular Chemistry. G. Wipff, editor. Kluwer Academic Publishers, Boston. 457–475.

Eriksson, M., T. Härd, and L. Nilsson. 1995. Molecular dynamics simulations of the glucocorticoid receptor DNA-binding domain in complex with DNA and free in solution. *Biophys. J.* 68:402–426.

Eriksson, M. A. L., and L. Nilsson. 1995. Structure, thermodynamics and cooperativity of the glucocorticoid receptor DNA-binding domain in complex with different response elements. Molecular dynamics simulation and free energy perturbation study. *J. Mol. Biol.* 253:453–472.

Finch, J. T., L. C. Lutter, D. Rhodes, R.-J. Brown, B. Ruston, M. Levitt, and A. Klug. 1977. Structure of nucleosome core particles of chromatin. *Nature.* 69:29–36.

Fragoso, G., S. John, M. S. Roberts, and G. L. Hager. 1995. Nucleosome positioning on the MMTV LTR results from the frequency-biased occupancy of multiple frames. *Genes Dev.* 9:1933–1947.

Freedman, L. P., B. F. Luisi, Z. R. Korszun, R. Basavappa, P. B. Sigler, and K. R. Yamamoto. 1988. The function and structure of the metal coordination sites within the glucocorticoid receptor DNA binding domain. *Nature.* 34:543–546.

Gewirth, D. T., and P. Sigler. 1995. The basis for half-site specificity explored through a non-cognate steroid receptor-DNA complex. *Nature Struct. Biol.* 2:386–394.

Gorin, A. A., V. B. Zhurkin, and W. K. Olson. 1995. B-DNA twisting correlates with base-pair morphology. *J. Mol. Biol.* 247:34–48.

Grubmüller, H., H. Heller, A. Windemuth, and K. Schulten. 1991. Generalized Verlet algorithm for efficient molecular dynamics simulations with long-range interactions. *Mol. Simulation.* 6:121–142.

Harris, L. F., M. R. Sullivan, P. D. Popken-Harris, and D. F. Hickok. 1994. Molecular dynamics simulations in solvent of the glucocorticoid receptor protein in complex with a glucocorticoid response element DNA sequence. *J. Biomol. Struct. Dyn.* 12:249–270.

Hayes, J. J., D. Clark, and A. P. Wolffe. 1990. The structure of DNA in a nucleosome. *Proc. Natl. Acad. Sci. USA.* 88:6829–6833.

Humphrey, W. F., A. Dalke, and K. Schulten. 1996. VMD—visual molecular dynamics. *J. Mol. Graph.* 14:33–38.

Jayaram, B., and D. Beveridge. 1996. Modelling DNA in aqueous solutions—theoretical and computer simulation studies on the ion atmosphere of DNA. *Annu. Rev. Biophys. Biomol. Struct.* 25:367–394.

Jorgensen, W. L., J. Chandrasekhar, J. D. Madura, R. W. Impey, and M. L. Klein. 1983. Comparison of simple potential functions for simulating liquid water. *J. Chem. Phys.* 79:926–935.

Kabsch W. 1976. A solution for the best rotation to relate two sets of vectors. *Acta Crystallogr. A.* 32:922–923.

Klug, A., and D. Rhodes. 1980. Helical periodicity of DNA determined by enzyme digestion. *Nature.* 286:573–578.

Kothekar, V., and A. Kotwal. 1992. Molecular mechanics simulation of the interaction of the estrogen receptor with estrogen regulatory element. *Indian J. Biochem. Biophys.* 29:322–329.

Levitt, M. 1982. Computer simulation of DNA double-helix dynamics. Cold Spring Harb. Symp. Quant. Biol. 47:251–262.

Luisi, B. F., W. X. Xu, Z. Otwinowski, L. P. Freedman, K. R. Yamamoto, and P. B. Sigler. 1991. Crystallographic analysis of the interaction of the glucocorticoid receptor with DNA. *Nature.* 352:497–505.

MacKerell, A., Jr., J. Wiorkiewicz-Kuczera, and M. Karplus. 1995. An all-atom empirical energy function for the simulation of nucleic acids. *J. Am. Chem. Soc.* 117:11946–11975.

Martinez, E., and W. Wahli. 1991. Characterization of hormone response elements. *In* Nuclear Hormone Receptors. M. G. Parker, editor. Academic Press, London and San Diego. 125–154.

McConnell, K. J., R. Nirmala, M. A. Young, G. Ravishanker, and D. L. Beveridge. 1994. A nanosecond molecular dynamics trajectory for a B DNA double helix: evidence for substates. *J. Am. Chem. Soc.* 116: 4461–4462.

Mymryk, J. S., and T. K. Archer. 1995. Dissection of progesterone receptor-mediated chromatin remodeling and transcriptional activation in vivo. *Genes Dev.* 9:1366–1376.

Nardulli, A. M., and D. J. Shapiro. 1992. Binding of the estrogen receptor DNA-binding domain to the estrogen response element induces DNA bending. *Mol. Cell. Biol.* 12:2037–2042.

Nelson, M., W. Humphrey, A. Gursoy, A. Dalke, L. Kalé, R. D. Skeel, and K. Schulten. 1996. NAMD—a parallel, object-oriented molecular dynamics program. *J. Supercomput. Appl.* 10:251–268, 1996.

Noll, M. 1974. Subunit structure of chromatin. *Nucleic Acids Res.* 1:1573–1578.

Olson, W. K. 1996. Simulating DNA at low resolution. *Curr. Opin. Struct. Biol.* 6:242–256.

Petz, L. H., A. M. Mardrelli, J. Kim, K. B. Horvitz, L. P. Freedman, and D. J. Shapiro. 1997. DNA bending is induced by binding of the glucocorticoid receptor DNA binding domain and the progesterone receptors to their response element. *J. Steroid Biochem. Mol. Biol.* In press.

Perlmann, T., and O. Wrange. 1988. Specific glucocorticoid receptor binding to DNA reconstituted in a nucleosome. *EMBO J.* 7:3073–3079.

Piña, B., U. Brüggemeier, and M. Beato. 1990. Nucleosome positioning modulates accessibility of regulatory proteins to the mouse mammary tumor virus promoter. *Cell.* 60:719–731.

Polach K. J., and J. Widom. 1995. Mechanism of protein access to specific DNA sequences in chromatin: a dynamic equilibrium model for gene regulation. *J. Mol. Biol.* 254:130–149.

Puhl, H. L., and M. J. Behe. 1993. Structure of nucleosomal DNA at high salt concentrations as probed by hydroxyl radical. *J. Mol. Biol.* 229: 827–832.

Rankin, W., and J. Board. 1995. A portable distributed implementation of the parallel multipole tree algorithm. *In* Proceedings, Fourth IEEE

International Symposium on High Performance Distributed Computing, IEEE Computer Society Press, 17–22.

Ravishanker, G., S. Swaminathan, D. L. Beveridge, R. Lavery, and H. Sklenar. 1989. Conformational and helicoidal analysis of 30 psec of molecular dynamics on the d(CGCGAATTCGCG) double helix. *J. Biomol. Struct. Dyn.* 6:669–699.

Record M. T., T. M. Lohman, and P. DeHaseth. 1976. Ion effects on ligand-nucleic acid interactions. *J. Mol. Biol.* 107:145–158.

Richard-Foy, H., and G. L. Hager. 1987. Sequence-specific positioning of nucleosomes over the steroid-inducible MMTV promoter. *EMBO J.* 6:2321–2328.

Richmond, T. J., J. T. Finch, B. Rushton, D. Rhodes, and A. Klug. 1984. Structure of the nucleosome core particle at 7 Å resolution. *Nature.* 311:532–537.

Roberts, M. S., G. Gragoso, and G. L. Hager. 1995. Nucleosomes reconstituted in vitro on mouse mammary tumor virus B region DNA occupy multiple translational and rotational frames. *Biochemistry.* 34: 12470–12480.

Sabbah, M., S. L. Ricousse, G. Redeuith, and E. Baulieu. 1992. Estrogen receptor-induced bending of the *Xenopus* vitellogen in A_2 gene hormone response element. *Biochem. Biophys. Res. Commun.* 185:944–952.

Sandmann, C., F. Cordes, and W. Saenger. 1996. Structure model of a complex between the factor for inversion stimulation (FIS) and DNA: modeling protein-DNA complexes with dyad symmetry and known protein structures. *Proteins Struct. Funct. Genet.* 25:486–500.

Schwabe, J. W. R., L. Chapman, J. T. Finch, and D. Rhodes. 1993. The crystal structure of the estrogen receptor DNA-binding domain bound to DNA: how receptors discriminate between their response elements. *Cell.* 75:567–578.

Schwabe, J. W. R., L. C. Chapman, and D. Rhodes. 1995. The oestrogen receptor recognizes an imperfectly palindromic response element through an alternative side-chain conformation. *Structure.* 3:201–213.

Sivolob, A. V., and S. N. Khrapunov. 1995. Translational positioning of nucleosomes on DNA: the role of sequence dependent isotropic DNA bending stiffness. *J. Mol. Biol.* 247:918–931.

Sklenar, H., C. Etchebest, and R. Lavery. 1989. The definition of generalized helicoidal parameters and of axis of curvature for irregular nucleic acids. *Proteins Struct. Funct. Genet.* 6:46–60.

Travers, A. A. 1987. DNA bending and nucleosome positioning. *Trends Biochem. Sci.* 12:108–112.

Truss, M., J. Bartsch, A. Schelbert, R. J. G. Haché, and M. Beato. 1995. Hormone induces binding of receptors and transcription factors to a rearranged nucleosome on the MMTV promoter in vivo. *EMBO J.* 14:1737–1751.

Watanabe, M., and M. Karplus. 1993. Dynamics of molecules with internal degrees of freedom by multiple time-step methods. *J. Chem. Phys.* 99:8063–8074.

Yang, L. Q., and B. M. Pettitt. 1996. B to A transition of DNA on the nanosecond time scale. *J. Phys. Chem.* 100:2564–2566.

Young, M. A., G. Ravishankar, D. L. Beveridge, and H. M. Berman. 1995. Analysis of local helix bending in crystal structures of DNA oligonucleotides and DNA-binding protein complexes. *Biophys. J.* 68: 2454–2468.